Available online at www.sciencedirect.com
SCIENCE DIRECT
NDT&E International 39 (2006) 205–216
NDT&E international
www.elsevier.com/locate/ndteint

Simulations of harmonic and pulsed ultrasonic polar scans

Nico F. Declercq*, Joris Degrieck, Oswald Leroy

Department of Mechanical Construction and Production, Soete Laboratory, Ghent University, Sint Pietersnieuwstraat 41, B-9000 Ghent, Belgium

Available online 22 August 2005

Abstract

Numerous experiments [1–5] have shown that ultrasonic polar scans are a promising tool for non-destructive characterization of fiber reinforced composites. However, because of the requirement to invert experimental data for extracting quantitative information [5], numerical simulations are mandatory. Such simulations have been developed before for single layered fiber reinforced composites. Nevertheless, since the vast majority of composites are multi-layered, the development of extended numerical models is needed. Such model is presented; together with a presentation of numerical simulations of ultrasonic polar scans for multi-layered composites. It is also shown that the polar scan of a fabric reinforced composite is quite different from a polar scan of (0/90°)-stacked unidirectional layers.

Furthermore, the difference between a polar scan for an incident harmonic wave and for an incident pulse is shown.

Keywords: Ultrasonic polar scans; Composites; Fatigue; Anisotropy; Lamb waves; pulse

1. Introduction

The principle of lowest possible mass for best suited stiffness and strength is the driving force behind the tailoring of high quality composites and the manufacturing of composite structures. This objective can only be achieved if it comes together with characterization during manufacturing and service life. Because destructive measurements are expensive, time consuming and mostly impossible, the application of ultrasound to this end is appropriate and its possibilities have been investigated for several years by various research groups [6–18].

The strength, stiffness, and the specific mass of composites are determined by the properties and the relative fractions of their constituents, by the physical structure of the composite (unidirectional, fabric,…), by the processing parameters, and by numerous sorts of defects and anomalies that can exist within these materials.

The use of ultrasonic techniques in nondestructive testing and characterization of materials is widely accepted, the oldest of which is perhaps the classical C-scan to detect and localize certain defects. Even though the classical C-scan has proved to be well suited for the task of detecting defects, an extension to more sophisticated means of measurements is necessary especially if characterization of the stiffness is requested. On fiber reinforced composite plates, this can only be performed if oblique incidence is considered as well.

An ‘ultrasonic polar scan’ is performed on a laminate immersed in water and investigates anisotropic mechanical features of the laminate exploiting its influence on obliquely incident sound. Nevertheless, contrary to most established methods of ultrasonic nondestructive characterization methods for fiber reinforced composite plates, utilizing time of flight measurements [9–16], or even spectroscopy [8], the ultrasonic polar scan uses the amplitude of transmitted (or if necessary reflected) sound, which results from sound impinging the plate from every direction above the plate and is relatively simple to measure.

Because a polar scan registers sound amplitudes on a small spot, it actually represents a local fingerprint of the plate under investigation. The characteristic pattern of such a ‘fingerprint’ consists in fact of a set of rings, showing considerably less intensity than elsewhere on the registered polar scan. The rings are physically connected [19] to generated critical waves in the plate, such as leaky Rayleigh waves, leaky Lamb waves or even lateral waves [20–32]. Hence, they almost directly clarify the mechanical anisotropy and the stiffness of the investigated spot.

* Corresponding author. Fax: +32 9 264 3587.
E-mail addresses: nicof.declercq@ugent.be (N.F. Declercq), declercq@ieee.org (N.F. Declercq).

0963-8695/$ - see front matter © 2005 Elsevier Ltd. All rights reserved.
doi:10.1016/j.ndteint.2005.07.004

It has been shown before [1–4,33,34] that the 'ultrasonic polar scan' is a highly recommended and convenient to use technique for the characterization of the fiber direction, the orthotropic stiffness, and for the extraction of information about porosity, resin fraction, etcetera.

Because fatigue damage induces stiffness reduction, it has been shown that polar scans are also excellent tools to monitor fatigue damage [35].

The present paper focuses on the theoretical modeling of ultrasonic polar scans. The last part of the paper presents some numerical examples of ultrasonic polar scans, for incident harmonic waves as well as for an incident pulse. The numerical method outlined below, though not new by itself [39], but for the first time deployed for simulating ultrasonic polar scans, is based on the so called direct method and does not imply sophisticated matrix methods [36–37]. The technique is deterministic and is not built on the Floquet wave principle [38] for periodically layered systems.

2. The effect of orthotropy on elasticity

In what follows, we apply the double suffix notation convention of Einstein. The dynamics of an anisotropic material is described [39] by

$$\frac{\partial \sigma_{ij}}{\partial r_j} = \rho \frac{\partial^2 u_i}{\partial t^2} \tag{1}$$

while the generalized Hooke's law, taking into account symmetry properties which are due to the analytical feature of the strain energy and the symmetric nature of the stress and strain tensors, is given by

$$\begin{bmatrix} \sigma_{11} \\ \sigma_{22} \\ \sigma_{33} \\ \sigma_{23} \\ \sigma_{13} \\ \sigma_{12} \end{bmatrix} = \begin{bmatrix} C_{11} & C_{12} & C_{13} & C_{14} & C_{15} & C_{16} \\ C_{12} & C_{22} & C_{23} & C_{24} & C_{25} & C_{26} \\ C_{13} & C_{23} & C_{33} & C_{34} & C_{35} & C_{36} \\ C_{14} & C_{24} & C_{34} & C_{44} & C_{45} & C_{46} \\ C_{15} & C_{25} & C_{35} & C_{45} & C_{55} & C_{56} \\ C_{16} & C_{26} & C_{36} & C_{46} & C_{56} & C_{66} \end{bmatrix} \begin{bmatrix} e_{11} \\ e_{22} \\ e_{33} \\ 2e_{23} \\ 2e_{13} \\ 2e_{12} \end{bmatrix} \tag{2}$$

Further symmetry considerations [39] due to orthotropy result in

$$C_{14} = C_{24} = C_{34} = C_{15} = C_{25} = C_{35} = C_{16} = C_{26} = C_{36} = C_{45} = C_{46} = C_{56} = 0 \tag{3}$$

In Engineering, orthotropic materials are often characterized by engineering constants, i.e. the Young's moduli E_{11}, E_{22} and E_{33}, the Poisson coefficients ν_{23}, ν_{13} and ν_{12}, and the shear moduli G_{23}, G_{13} and G_{12}.

Then

$$\begin{bmatrix} C_{11} & C_{12} & C_{13} & 0 & 0 & 0 \\ C_{12} & C_{22} & C_{23} & 0 & 0 & 0 \\ C_{13} & C_{23} & C_{33} & 0 & 0 & 0 \\ 0 & 0 & 0 & C_{44} & 0 & 0 \\ 0 & 0 & 0 & 0 & C_{55} & 0 \\ 0 & 0 & 0 & 0 & 0 & C_{66} \end{bmatrix} = \begin{bmatrix} 1/E_{11} & -\nu_{12}/E_{11} & -\nu_{13}/E_{11} & 0 & 0 & 0 \\ -\nu_{21}/E_{22} & 1/E_{22} & -\nu_{23}/E_{22} & 0 & 0 & 0 \\ -\nu_{31}/E_{33} & -\nu_{32}/E_{33} & 1/E_{33} & 0 & 0 & 0 \\ 0 & 0 & 0 & 1/G_{23} & 0 & 0 \\ 0 & 0 & 0 & 0 & 1/G_{31} & 0 \\ 0 & 0 & 0 & 0 & 0 & 1/G_{12} \end{bmatrix}^{-1} \tag{4}$$

with

$$\nu_{32} = \nu_{23} \frac{E_{33}}{E_{22}} \tag{5}$$

$$\nu_{31} = \nu_{13} \frac{E_{33}}{E_{11}} \tag{6}$$

$$\nu_{21} = \nu_{12} \frac{E_{22}}{E_{11}} \tag{7}$$

and

$$G_{ij} = G_{ji} \tag{8}$$

3. The propagation of bulk plane waves

We represent the acoustic field inside and outside the composite as a superposition of all possible bulk modes given an incident bulk wave [40,41]. Therefore we are mainly interested in a resulting field and do not attempt to study sound rays and point sources in a composite [42,43]. The reverse Voigt procedure transforms the stiffness tensor C_{mn} of rank 2 to the stiffness tensor C_{ijkl} of rank 4 as ($1 \rightarrow 11$), ($2 \rightarrow 22$), ($3 \rightarrow 33$), ($4 \rightarrow 23 = 32$), ($5 \rightarrow 13 = 31$) and ($6 \rightarrow 12 = 21$). When necessary, the intrinsic stiffness constants $c_{ijkl} = c^I_{ijkl}$ can be transformed into stiffness constants $c_{ijkl} = c^R_{ijkl}$ in coordinates corresponding to a rotated (laboratory) system as follows

$$c^R_{ijkl} = R_{im} R_{jn} R_{kp} R_{lq} c^I_{mnpq} \tag{9}$$

where R_{ij} are the entries of the rotation matrix for a rotation from the intrinsic lattice coordinate system to the laboratory coordinate system.

Eq. (1) then becomes

$$\rho \frac{\partial^2 u_i}{\partial t^2} = c_{ijkl} \frac{\partial^2 u_l}{\partial x_j \partial x_k} \tag{10}$$

A plane wave solution of (10) is of the form

$$u_i = U_i \exp i(n_j r_j - \omega t) \tag{11}$$

where **n** is the wave vector. If this is entered in (10), straightforward calculations then result in

$$\left(\frac{1}{\rho} c_{ijkl} n_k n_j - \omega^2 \delta_{il}\right) U_l = 0 \tag{12}$$

The latter equation is called Christoffel's equation [39, 44–47]. It relates the slowness n/ω and the polarization **U** to the propagation direction and is solved by demanding nontrivial solutions, followed by the determination of the corresponding eigenvectors.

4. The scattering of plane waves

4.1. Snell's law

If sound inside the bulk of the composite laminate results from impinging plane waves (denoted by superscript 'inc'), Snell's law must be taken into account which, for interfaces perpendicular to n_3, states that

$$n_1 = n_1^{\text{inc}} \quad \text{and} \quad n_2 = n_2^{\text{inc}} \tag{13}$$

Then, requiring nontrivial solutions, (12) leads to a sixth degree polynomial equation of the form in which β represents n_3.

$$\beta^6 + B_5\beta^5 + A_4\beta^4 + B_3\beta^3 + A_2\beta^2 + B_1\beta + A_0 = 0 \tag{14}$$

Furthermore, it can be shown [39] that the presence of symmetry higher than or equal to monoclinic symmetry (as is the case for orthotropy) results in $B_j = 0$ whence three independent solutions exist

$$\beta_2 = -\beta_1 \quad \beta_4 = -\beta_3 \quad \beta_6 = -\beta_5 \tag{15}$$

4.2. Continuity of normal stress and displacement

For a plate immersed in water, two different continuity conditions are involved. The water/solid interface is determined by continuity of normal stress and normal displacement, hence along the interface,

$$u_3^{\text{water}} = u_3^{\text{solid}} \tag{16}$$

and

$$\sigma_{i3}^{\text{water}} = \sigma_{i3}^{\text{solid}}, \quad i = 1, 2, 3 \tag{17}$$

It is implicitly understood that water does not carry shear waves and therefore, Eq. (10) does involve $\sigma_{13}^{\text{solid}} = \sigma_{23}^{\text{solid}} = 0$ along the water/solid interface. This is automatically taken into account by expressing the sound field in water in terms of the acoustic potential $\varphi = A\exp i(n_j r_j - \omega t)$ with the particle displacement written as $\mathbf{u} = \text{grad}\varphi$ [56].

The solid/solid interface(s) are determined by the continuity of the displacement vector and continuity of normal stress, hence along the interface(s)

$$u_i^{\text{solid}} = u_i^{\text{solid}}, \quad i = 1, 2, 3 \tag{18}$$

and

$$\sigma_{i3}^{\text{solid}} = \sigma_{i3}^{\text{solid}}, \quad i = 1, 2, 3 \tag{19}$$

By taking into account the appropriate continuity conditions and by applying the discussion of Section 4.1, one is able to simulate a polar scan by building the continuity matrix and extract the amplitudes for the different bulk wave components in the composite and in the surrounding liquid. The procedure that we have developed automatically builds the complete continuity matrix no matter how many layers there are involved. Furthermore, we consider the composite plate as it is and do not use any simplification based on the periodicity of the layers [38,48].

5. The principle of a polar scan

A classical C-scan is formed by registering the reflected or transmitted signal on many spots on the laminate surface, by applying normal incidence. Most often, C-scans are used to detect material defects and eventually to find out the 3D locations of such defects. Lately, some attempts have been undertaken to unveil the fiber direction by means of C-scans. However, the reported methods can only be used if sufficient microscopic material defects exist on the fiber/matrix interface or if the fibers are not equally distributed within the matrix.

A polar scan differs from a classical C-scan in that the transducer is not constantly held perpendicular to the interface. On the contrary, a polar scan exploits oblique incidence and measures the reflected or transmitted specular sound resulting from sound that is subsequently incident from all possible directions from above the plate. As is seen in Fig. 1, the incidence direction is defined by (θ, φ). The reflected/transmitted amplitude is then registered in a polar diagram where each spot corresponds to a certain ($\theta+\pi$,φ) and represents the amplitude for that direction. The radius in

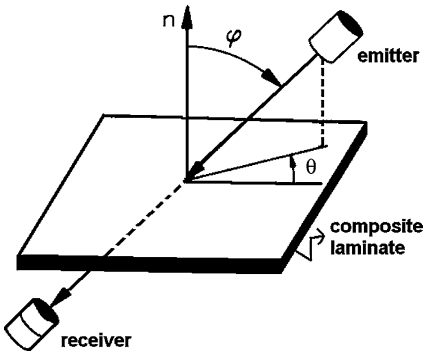

Fig. 1. The position of the transducers in a polar scan.

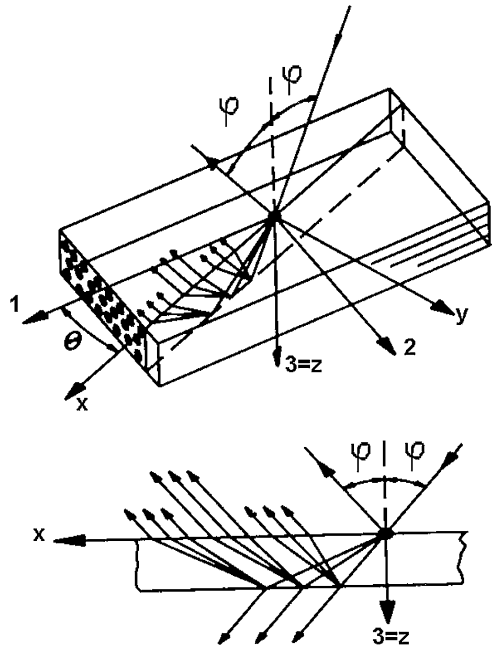

Fig. 2. The complicated interaction of an incident plane wave with a single layered composite plate. Each scattering generates 3 propagation modes in the plate and 1 in the liquid.

the registrations corresponds to ϕ, whereas the polar angle denotes θ. The grey scale is a measure for the received amplitude. Physically, the process of sound impinging the plate and traveling inside the plate, being scattered once and again by the different interfaces, is a very complicated phenomenon [42,43], cfr. Fig. 2. However, for harmonic incident waves and for a pulse (we may always consider a pulse as a superposition of harmonic waves), a 'standing wave pattern (for the particle displacement as a function of the depth)' is formed inside the plate, which is modeled by demanding only six modes (the six coming from Christoffel's Eq. (12)) propagating in each layer. This standing wave pattern may result in some kind of an eigen-vibration of the plate. If this occurs, this pattern is called a quasi Lamb wave. The term 'quasi' is used in anisotropic materials and denotes the fact that these waves are a generalized form of Lamb waves that do exist in isotropic materials. Only along symmetry axes, the term 'quasi' could be replaced by 'pure'. A similar expression is later on used for 'quasi longitudinal' and 'quasi shear' waves. The quasi polarization only corresponds to a pure polarization as in isotropic materials, along axes of symmetry. It is characterized by a reflection/transmission coefficient tending to zero. This results in 'dark regions' in the registered polar scan.

The position and the characteristics of these regions are determined by the physical parameters of the plate, such as the thickness of the layers, the density, the stiffness coefficients and the damping. Ultrasonic polar scans form therefore an excellent tool for monitoring these physical properties. The interpretation of a polar scan is a difficult task. However, in the case of thick plates, the only patterns that do appear are due to bulk critical angles. For reasons of explanatory simplicity we solely focus on this case. Snell's law for critical waves is as follows

$$\sin(\varphi_{\text{crit}})|_{\theta} = v_l/v_{\text{crit}}(\rho, C_{ij}, \theta) \tag{20}$$

where v_l is the plane wave velocity in the liquid and v_{crit} is the velocity of the critical bulk wave.

If a certain contour in one direction is wider than in other directions, this means that the velocity in the 'wider' direction is lower than in the other direction. For example the velocities of quasi longitudinal waves (corresponding to the inner contour of a polar scan) traveling along the in-plane axes of orthotropy are given by $\sqrt{C_{11}/\rho}$ and $\sqrt{C_{22}/\rho}$, respectively.

Hence, regarding Eq. (20), the directions of highest stiffness produce the smallest critical angles for quasi longitudinal waves. Even though the contours of polar scans for thin plates are much more difficult to interpret, the basic idea remains unchanged. Furthermore, whenever a pulse is used instead of a harmonic wave, the remaining patterns of a polar scan correspond quite well to patterns that are caused by bulk lateral waves. That is because the dispersive nature of Lamb waves, i.e. a frequency dependent velocity, results in phase canceling for a pulse (because each plane wave component within the pulse, results in a largely different complex reflection coefficient), whereas, bulk waves are not dispersive and their effects are not canceled out.

6. Numerical examples for harmonic waves

Hereafter, each polar scan is simulated for a 1-mm thick fiber reinforced plate and an ultrasonic sound frequency of 5 MHz. For multilayered systems, we consider layers of equal thickness. Furthermore the calculations are performed using realistic values for the materials properties. This involves the presence of damping and is determined by means of complex valued stiffness elements [49–55].

6.1. Single-layered unidirectional carbon/epoxy fiber reinforced composites

The physical parameters of the carbon epoxy composite that are exploited here, can be found in Table 1 (type A). Fig. 3 presents the numerical simulation of an ultrasonic polar scan (in reflection) for a single layered unidirectional carbon/epoxy fiber reinforced composite. The fibers are oriented along the 0° polar direction. In that direction, it is indeed verified that the inner contour (which corresponds to the quasi longitudinal plane wave critical angle) is smallest, which is caused by the elevated stiffness along the fiber direction. The other contours are a result of generated quasi-Lamb waves and a result of generated lateral quasi-shear waves. Fig. 4 is equivalent to Fig. 3,

Table 1
Properties of one layer of: Carbon/Epoxy unidirectional fiber reinforced composites (Type A), Glass/Epoxy fabric fiber reinforced composites (Type B), FR4 (Type C)

Parameter	Type A	Type B	Type C
ρ (kg/m^3)	1525	1750	1925
E_{11} (MPa)	119,130 (1−0.0025i)	20,845(1−0.01i)	20,030(1−0.15i)
E_{22} (MPa)	8850(1−0.03i)	20,845(1−0.01i)	22,630(1−0.15i)
E_{33} (MPa)	10,000(1−0.03i)	8628(1−0.03i)	8628(1−0.005i)
ν_{23}	0.475(1−0.015i)	0.414(1−0.015i)	0.5(1−0.005i)
ν_{13}	0.275(1−0.01i)	0.414(1−0.01i)	0.5(1−0.005i)
ν_{12}	0.306(1−0.01i)	0.125(1−0.01i)	0.1793(1−0.08i)
G_{23} (MPa)	3000(1−0.05i)	2930(1−0.05i)	3930(1−0.04i)
G_{13} (MPa)	5000(1−0.02i)	2930(1−0.02i)	3930(1−0.04i)
G_{12} (MPa)	5500(1−0.03i)	3110(1−0.03i)	4781(1−0.15i)

except that here the ultrasonic polar scan in transmission is plotted. Due to damping, the overall amplitude is smaller, but characteristic contours are still visible.

6.2. Double layered cross-ply carbon/epoxy laminate (0/90°)

Each layer is characterized by physical parameters listed in Table 1 (type A). Figs. 5 and 6 represent the numerical simulations of ultrasonic polar scans on a double layered carbon/epoxy fiber reinforced composite with the top layer consisting of fibers in the 0° direction and the bottom layer built up by fibers in the 90° direction. The presence of both symmetries (one on top of the other), is clearly visible in the characteristic contours if compared to Figs. 3 and 4. Moreover, it is seen that the reflected pattern in the 0° polar direction is not equivalent to the pattern in the 90° polar direction.

6.3. Single layered fabric glass/epoxy reinforced composites

The physical properties of this composite are listed in Table 1 (type B). Figs. 7 and 8 are the simulations of ultrasonic polar scans on a fabric glass/epoxy reinforced composite. Even though the laminate also consists of fibers in epoxy resin, the actual stiffness is different from the cross-ply composite described above. Hence, only qualitative comparison is allowed. It is seen that the pattern in the 0° polar direction matches perfectly to the pattern in the 90° polar direction. It is clear that the patterns qualitatively differ strongly form those of Figs. 5 and 6. Hence, a single layered fabric fiber reinforced composite is quite different from a (0/90°) double layered fiber reinforced composite.

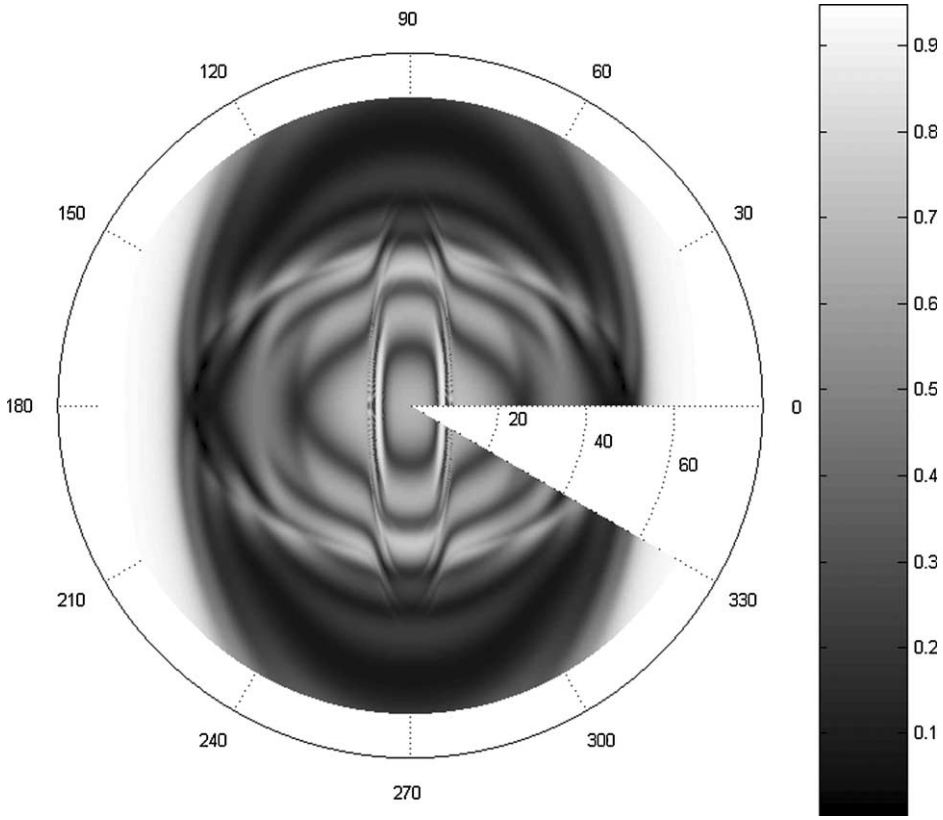

Fig. 3. Ultrasonic Polar Scan (harmonic, in reflection) of a single layered unidirectional fiber reinforced composite.

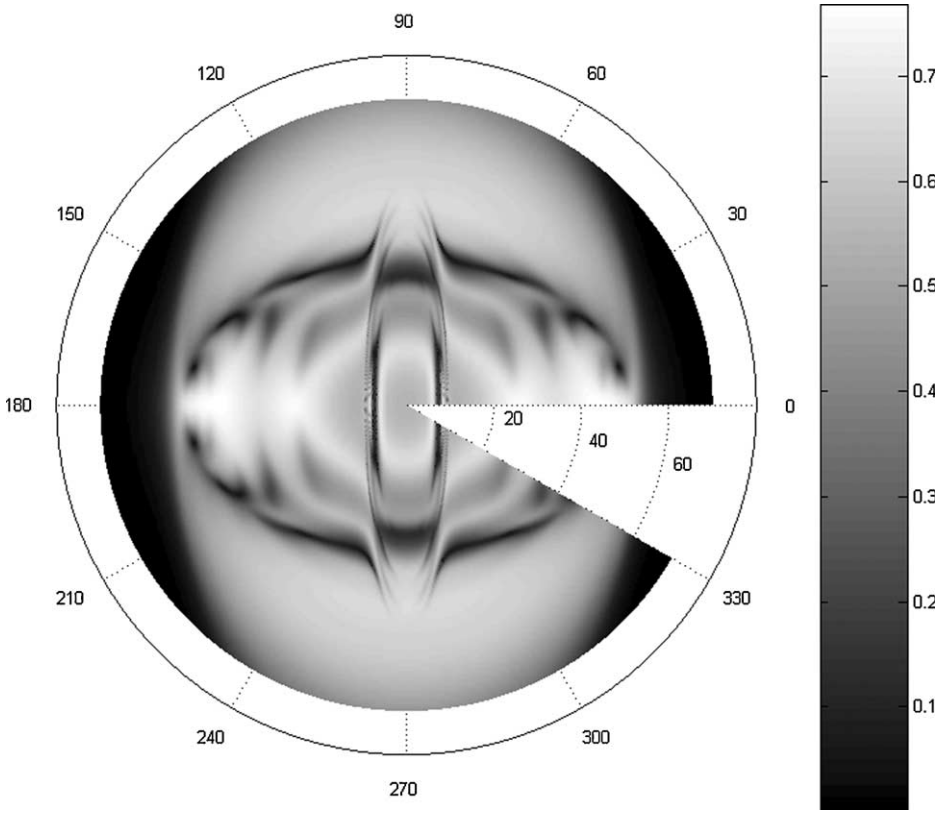

Fig. 4. Ultrasonic Polar Scan (harmonic, in transmission) of a single layered unidirectional fiber reinforced composite.

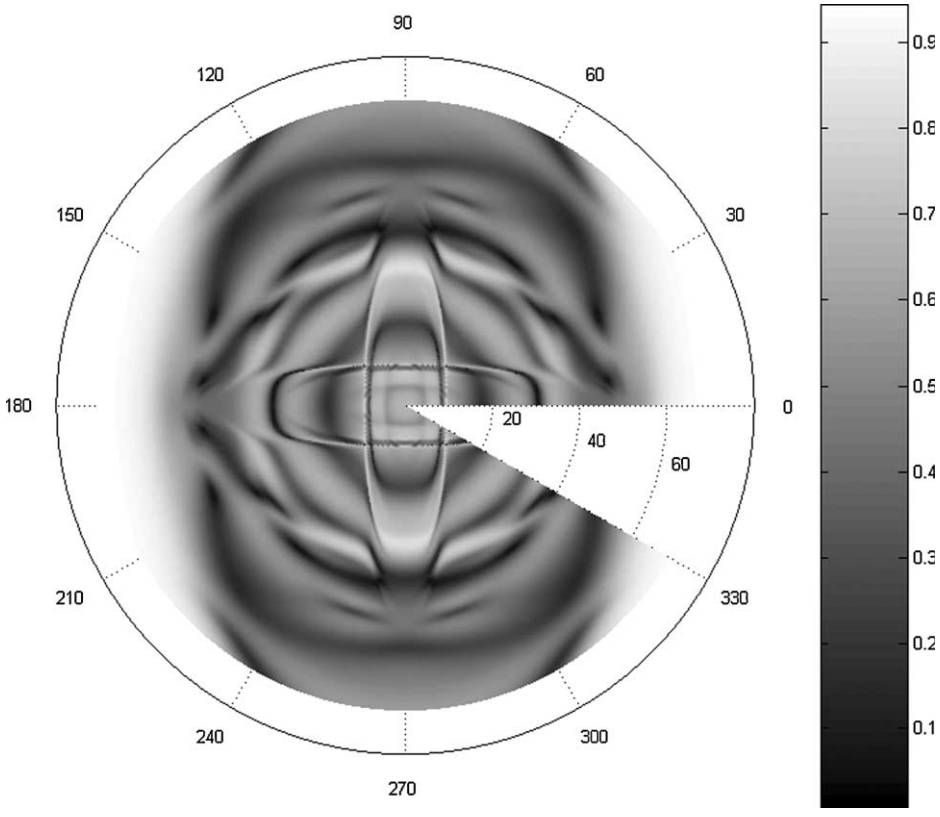

Fig. 5. Ultrasonic Polar Scan (harmonic, in reflection) of a double layered (0/90°) cross-ply laminate.

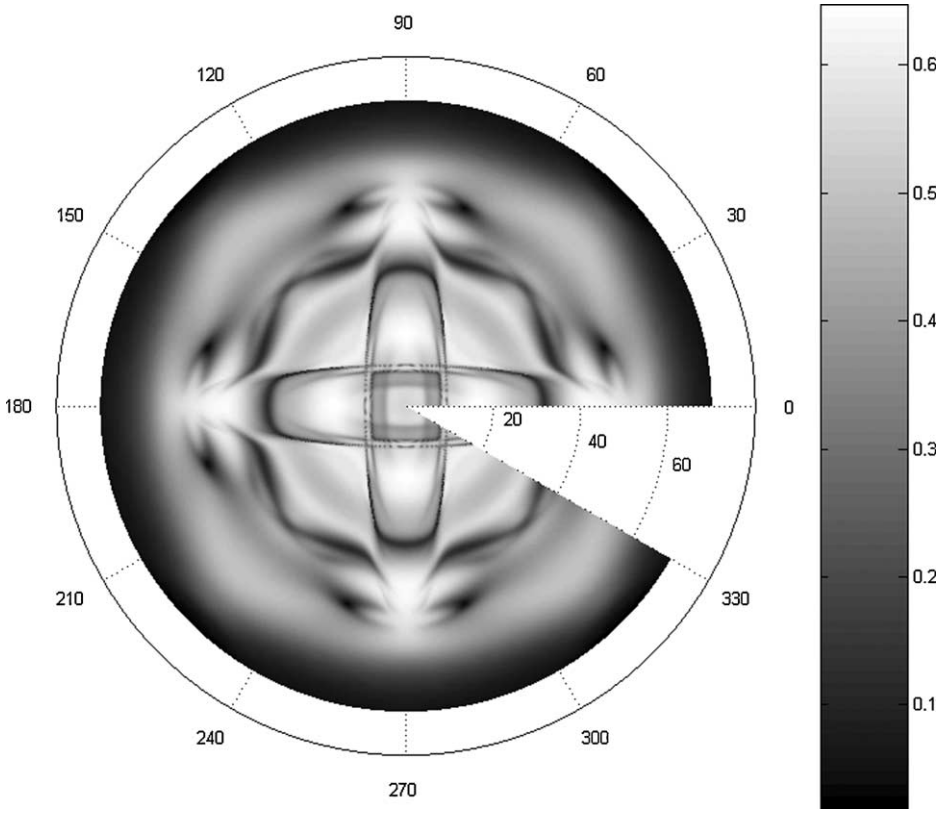

Fig. 6. Ultrasonic Polar Scan (harmonic, in transmission) of a double layered (0/90°) cross-ply laminate.

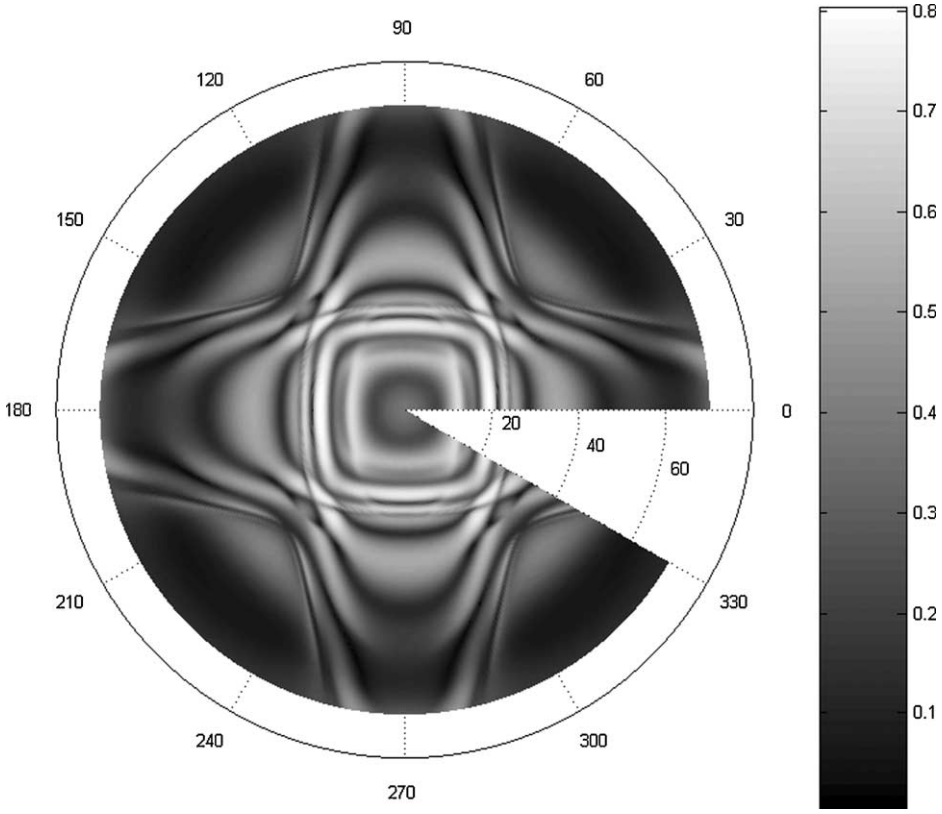

Fig. 7. Ultrasonic Polar Scan (harmonic, in reflection) of a single layered fabric reinforced composite.

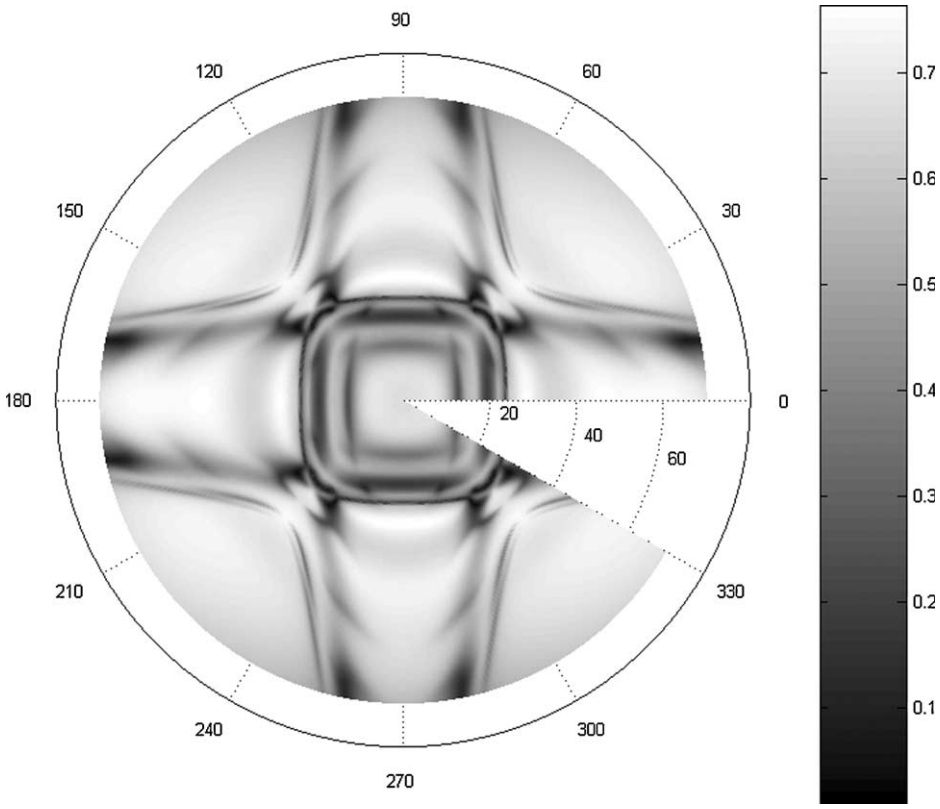

Fig. 8. Ultrasonic Polar Scan (harmonic, in transmission) of a single layered fabric reinforced composite.

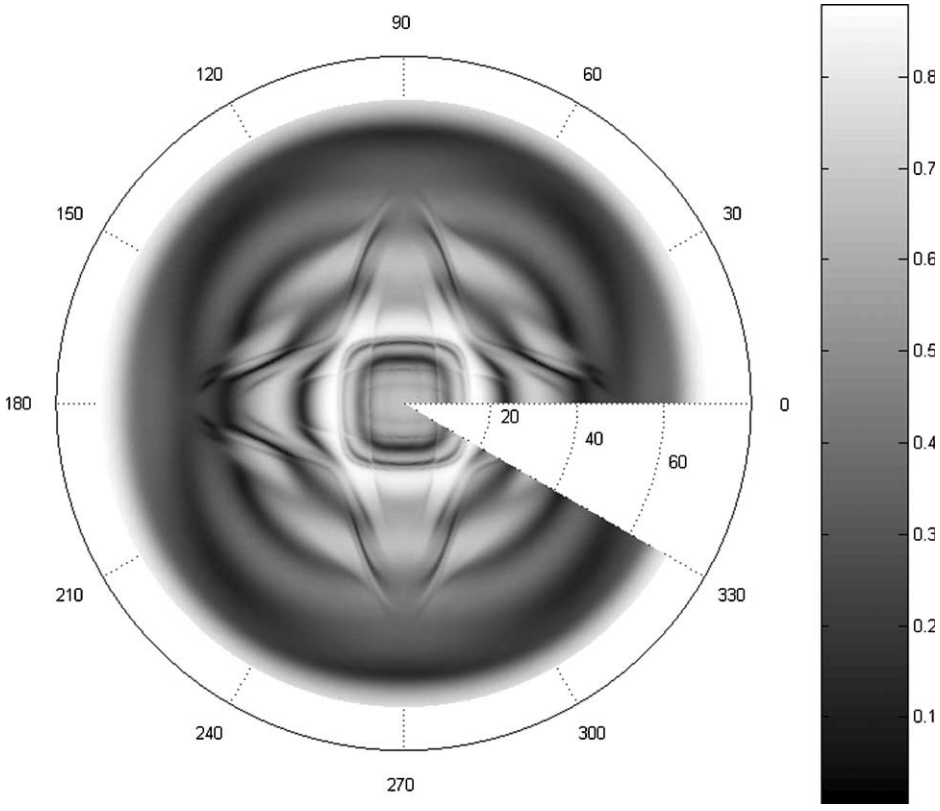

Fig. 9. Ultrasonic Polar Scan (harmonic, in reflection) of a cross-ply composite consisting of 10 (0/90°) stacked layers of unidirectional fiber reinforced material.

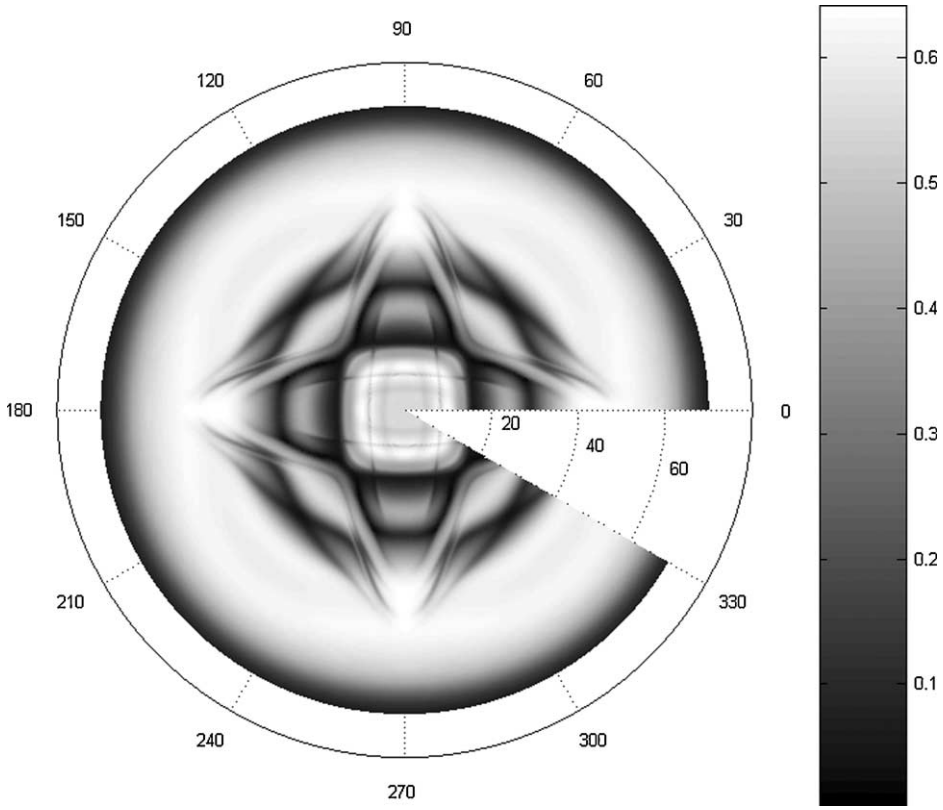

Fig. 10. Ultrasonic Polar Scan (harmonic, in transmission) of a cross-ply reinforced composite consisting of 10 (0/90°) stacked layers of unidirectional fiber reinforced material.

6.4. Multi-layered cross-ply carbon/epoxy laminate (0/90°)

Each layer is characterized by physical parameters listed in Table 1 (type A). In order to check the relevancy of the above statement that a fabric fiber reinforced composite is different from a (0/90°) stacked composite, we have decided to increase the number of layers to 10. The numerical result is seen in Figs. 9 and 10. Even though the number of layers is much larger, still there is a difference between the polar scans of Figs. 9 and 10 and the ones of Figs. 7 and 8. Even here, with a significantly increased number of stacked layers, the reflected pattern in the 0° polar direction still differs significantly from the pattern in the 90° polar direction. This finding is important since it is common for many researchers to model a fabric fiber reinforced composite as (0/90°) stacked layers of unidirectional material. It is obvious from the given result that this should be avoided.

7. Numerical example for a pulse

A FR4 composite laminate is a fabric glass fiber reinforced epoxy composite and is frequently used in electronic devices. Table 1 (type C) lists the material parameters of the FR4 laminate that is investigated here. We study the interaction of a pulse with the considered laminate. The considered pulse corresponds with a pulse that is generated by a Krautkrämer H5M shock wave probe [35] with a nominal frequency of 5 MHz and is given by

$$\frac{ft}{M}\cos(2\pi ft)\exp\left(-\left(\frac{ft}{p}\right)^2\right) \tag{21}$$

with $f=5$ MHz and $p=1.08$ and M a normalization constant. Expression (20) is plotted in Fig. 11. This signal is simulated by means of the Fourier transformation whence it is written as a superposition of harmonic plane waves.

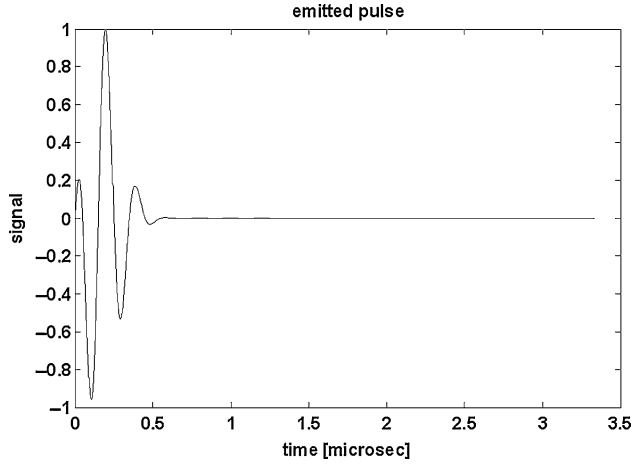

Fig. 11. The amplitude versus time profile of the impinging sound pulse.

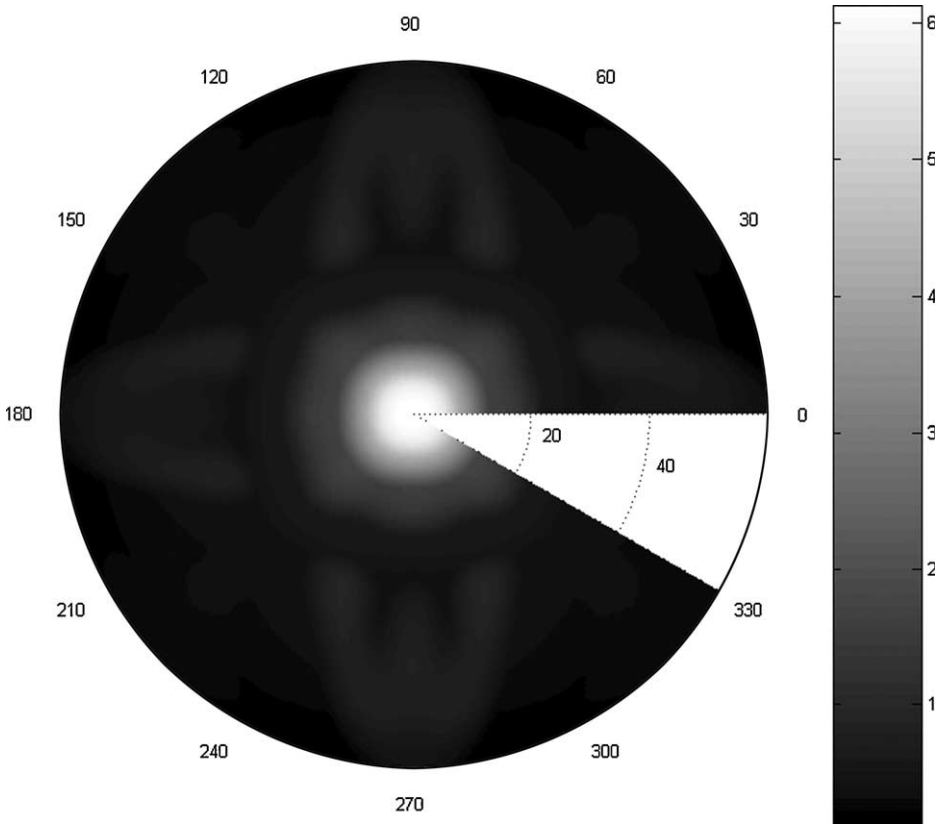

Fig. 12. simulation of ultrasonic polar scan (pulsed, in reflection) on a FR4 plate.

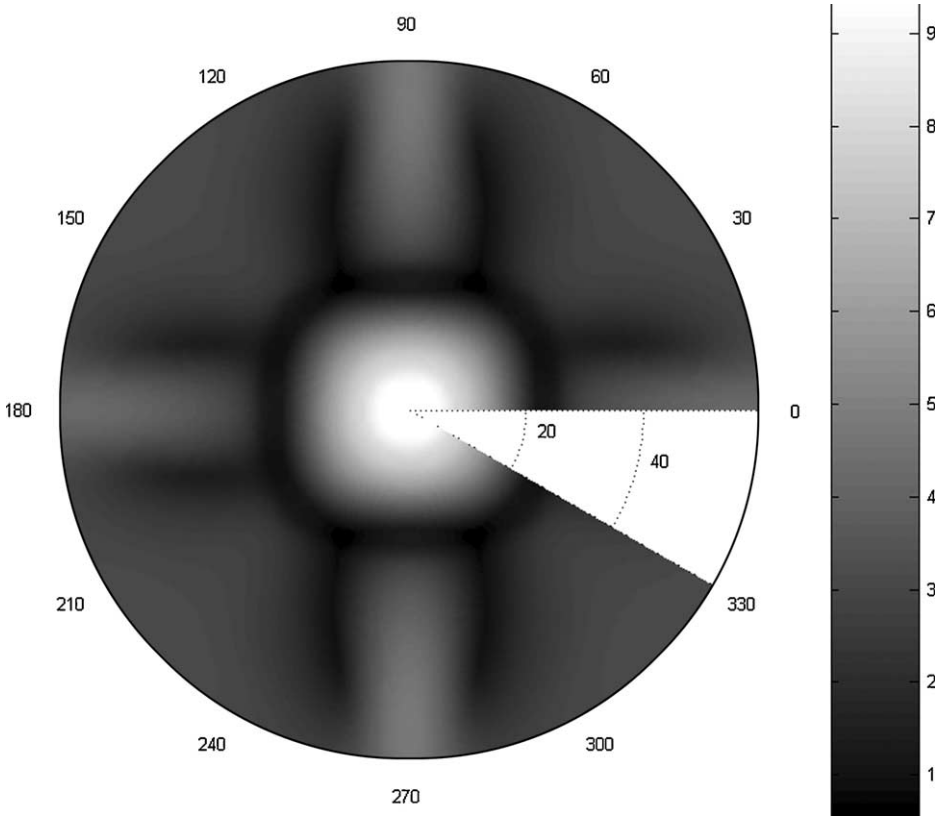

Fig. 13. simulation of ultrasonic polar scan (pulsed, in transmission) on a FR4 plate.

Each of them is interacting with the composite as described earlier and the consequential field is again the summation of the resulting fields caused by each individual harmonic wave. The reflected amplitude is then defined as the maximum output as a function of time. The exact instant when that maximum is reached as well as the maximum value itself depends on the angle of incidence. In a polar scan for an incident pulse, the maximum reflected or transmitted value is plotted as a function of each angle of incidence. For the FR4 composite, here for a thickness of 1.2 mm, the polar scan in reflection is given in Fig. 12, whereas, the one in transmission is given in Fig. 13. It is seen that no such complicated patterns appear as when an incident harmonic wave was considered (cfr. Fig. 8). As has been explained earlier, the reason for that is that the resulting patterns correspond to bulk critical angles and not to Lamb wave patterns.

8. Concluding remarks

It is shown how numerical simulations of polar scans are performed, starting from simple principles of mechanics and wave motion. Even though simulations on single layered fiber reinforced composites already existed, the theoretical model has been extended to multi-layered composites. As an excellent example, it has been shown that fabric fiber reinforced composites cannot be modeled sufficiently accurate by means of a model in which unidirectional fiber reinforced layers are stacked in large numbers in the 0° polar direction and the 90° polar direction. We have discussed polar scans for incident harmonic waves and an incident pulse. In the near future, the applied model will be further extended to crystals and also to pre-stressed composites. These numerical simulations, together with the upgraded and highly modernized experimental set up may become a means of characterizing the stiffness of anisotropic plates. It is the authors' purpose to develop an automated tool that applies a numerical/experimental inversion technique and to rebuild the experimental apparatus to meet in-field requirements. Due to the strong connection to stiffness, the developed technique is intended to monitor fatigue damage on composites, porosity, and resin fractions. Furthermore, it will be used to verify micro-mechanical models.

Acknowledgements

Nico F. Declercq is a Postdoctoral Fellow of the Research Foundation Flanders (F.W.O.-Vlaanderen, Belgium). The authors are also thankful to 'The Flemish Institute for the Promotion of the Scientific and Technological Research in Industry (I.W.T)' for financial support and to the 'Research Foundation Flanders (F.W.O.-Vlaanderen, Belgium)' for offering a travel grant to join the 3rd International Conference 'Emerging Technologies in Non-Destructive Testing', 26–28 May 2003, Thessaloniki, Greece, where the core of this paper has been presented.

References

[1] Van Dreumel WHM, Speijer JL. Nondestructive composite laminate characterization by means of ultrasonic polar scan. Mater Eval 1981; 39(15):922–5.
[2] Degrieck J, Van Leeuwen D. Simulatie van een ultrasone polaire scan van een orthotrope plaat. In: Proceedings of the 3rd Belgian national congres on theoretical and applied mechanics. Belgium: Liege University, 1994, p. 39–42. (in dutch)
[3] Degrieck J. Some possibilities of nondestructive characterization of composite plates by means of ultrasonic polar scans.. In: Van Hemelrijck D, Anastassopoulos A, editors. Non destructive testing. Balkema: Rotterdam; 1996. p. 225–36.
[4] Declercq NF, Degrieck J, Leroy O. Characterization of layered orthotropic materials using ultrasonic polar scans. In: Proceedings of the 2nd FTW PhD symposium. Belgium: Ghent University, 2001.
[5] Degrieck J, Declercq NF, Leroy O. Ultrasonic Polar scans as a possible means of nondestructive testing and characterization of composite plates. Insight-J Br Inst Non-Destr Test 2003;45(3): 196–201.
[6] Lavrentyev AI, Rokhlin SI. Determination of elastic moduli, density, attenuation, and thickness of a layer using ultrasonic spectroscopy at two angles. J Acoust Soc Am 1997;102(11):3467–77.
[7] Chu YC, Rokhlin SI. Comparative analysis of through-transmission ultrasonic bulk wave methods for phase velocity measurements in anisotropic materials. J Acoust Soc Am 1994;95(11):3204–12.
[8] Hsu DK, Hughes MS. Simultaneous ultrasonic velocity and sample thickness measurement and application in composites. J Acoust Soc Am 1992;92(2):669–75.
[9] Chu Y, Rokhlin SI. A method for determination of elastic constants of a unidirectional lamina from ultrasonic bulk velocity measurements on [0/90] cross-ply composites. J Acoust Soc Am 1994;96(1):342–52.
[10] Rokhlin SI, Huang W, Chu YC. Ultrasonic scattering and velocity methods for characterization of fibre-matrix interphases. Ultrasonics 1995;33(10):351–64.
[11] Deschamps M, Bescond C. Numerical method to recover the elastic constants from ultrasonic group velocities. Ultrasonics 1995;33(3): 205–11.
[12] Degtyar AD, Rokhlin SI. Comparison of elastic constant determination in anisotropic materials from ultrasonic group and phase velocity data. J Acoust Soc Am 1997;102(11):3458–66.
[13] Aristégui C, Baste S. Optimal recovery of the elasticity tensor of general anisotropic materials from ultrasonic velocity data. J Acoust Soc Am 1997;101(2):813–33.
[14] Aristégui C, Baste S. Optimal determination of the material symmetry axes and associated elasticity tensor from ultrasonic velocity data. J Acoust Soc Am 1997;102(3):1503–21.
[15] Enderby MD, Clarke AR, Patel M, Ogden P, Johnson AA. An automated ultrasonic immersion technique for the determination of three-dimensional elastic constants of polymer composites. Ultrasonics 1998;36:245–9.
[16] Reverdy F, Audoin B. Elastic constants determination of anisotropic materials from phase velocities of acoustic waves generated and detected by lasers. J Acoust Soc Am 2001;109(10):1965–72.
[17] Pluta M, Every AG, Grill W, Kim TJ. Fourier inversion of acoustic wave fields in anisotropic solids. Phys Rev; B 2003;B 67(14) [Art. No. 094117].

[18] Bescond C, Audoin B, Deschamps M, Qian M. Measurement by laser generated ultrasound of the stiffness tensor of an anisotropic material. Acta Acust United Ac 2002;88(1):50–8.
[19] Buchwald VT, Davis A. Surface waves in anisotropic elastic media. Nature 1961;191:899–900.
[20] Chimenti DE, Rokhlin SI. Relationship between leaky Lamb modes and reflection coefficient zeroes for a fluid-coupled elastic layer. J Acoust Soc Am 1990;88(3):1603–11.
[21] Buchwald VT. Rayleigh waves in anisotropic media. Quart J Mech Appl math 1961;XIV(9):461–9.
[22] Lim TC, Musgrave MJP. Stoneley waves in anisotropic media. Nature 1970;225:372.
[23] Nayfeh AH, Chimenti DE. Propagation of guided waves in fluid-coupled plates of fiber-reinforced composite. J Acoust Soc Am 1988; 83(10):1736–43.
[24] Dayal V, Kinra VK. Leaky lamb waves in an anisotropic plate. I: an exact solution and experiments. J Acoust Soc Am 1989;85(11): 2268–76.
[25] Chimenti DE, Martin RW. Nondestructive evaluation of composite laminates by leaky Lamb waves. Ultrasonics 1991;29:13–21.
[26] Ting TCT, Barnett DM. Classifications of surface waves in anisotropic elastic materials. Wave Motion 1997;26:207–18.
[27] Castaings M, Hosten B. The use of electrostatic, ultrasonic, air-coupled transducers to generate and receive Lamb waves in anisotropic, viscoelastic plates. Ultrasonics 1998;36:361–5.
[28] Moreno E, Acevedo P. Thickness measurement in composite materials using Lamb waves. Ultrasonics 1998;35:581–6.
[29] Jeong H, Hsu DK. Experimental analysis of porosity-induced ultrasonic attenuation and velocity change in carbon composites. Ultrasonics 1995;33(3):195–203.
[30] Jeong H. Multiple NDE techniques for the measurement of constituent volume fractions in metal matrix composites. Res Nondestr Eval 1997;9:41–57.
[31] Zou W, Holland S, Kim KY, Sachse W. Wideband high-frequency line-focus PVDF transducer for materials characterization. Ultrasonics 2003;41(3):157–61.
[32] Ben Amor M, Ben Ghozlen MH, Lanceleur P. Modelling of elastic waves generated at the interface between anisotropic media. Acta Acust United Ac 2003;89(9):625–31.
[33] Declercq NF., Degrieck J, Leroy O. Numerical simulations of ultrasonic polar scans on fiber reinforced composites. In Proceedings of the 29 Deutsche Jahrestagung für Akustik DAGA 2003. 18–20. March 2003, Aachen, Germany, 2003.
[34] Declercq NF, Degrieck J, Leroy O. Numerical simulations of ultrasonic polar scans. In: Van Hemelrijck D, Anastasopoulos A, Melanitis NE, editors. Emerging technologies in nondestructive testing. Lisse, 2004. Amsterdam: Swets and Zeitlinger; 2004. p. 75–80.
[35] Declercq NF, Degrieck J, Leroy O. On the influence of fatigue on ultrasonic polar scans of fiber reinforced composites. Ultrasonics 2004; (In press).
[36] Wang L, Rokhlin SI. Ultrasonic wave interaction with multi-directional composites: modeling and experiment. J Acoust Soc Am 2003;114(10):2582–95.
[37] Hosten B, Castaings M. Surface impedance matrices to model the propagation in multilayered media. Ultrasonics 2003;41(12):501–7.
[38] Potel C, Gatignol P, de Belleval JF. Energetic criterion for the radiation of Floquet waves in infinite anisotropic periodically multilayered media. Acta Acust united Ac 2001;87(3):340–51.
[39] Naefeh AH. Wave propagation in layered anisotropic media with applications to composites North Holland series in applied mathematics and mechanics 1995.
[40] Deschamps M, Hosten B. The effects of viscoelasticiy on the reflection and transmission of ultrasonic waves by an orthotropic plate. J Acoust Soc Am 1992;91(9):2007–15.
[41] Hosten B, Castaings M. Transfer matrix of multilayerd absorbing and anisotropic media. Measurements and simulations of ultrasonic wave propagation through composite materials. J Acoust Soc Am 1993; 94(3):1488–95.
[42] Kim KY, Zou W, Sachse W. Wave propagation in a wavy fiber-epoxy composite material: Theory and experiment. J Acoust Soc Am 1998; 103(10):2296–301.
[43] Lu XR, Kim KY, Sachse W. In situ determination of elastic stiffness constants of thick composites. Compt Sci Technol 1997;12:753–62.
[44] Pluta M, Schubert M, Jahny J, Grill W. Angular spectrum approach for the computation of group and phase velocity surfaces of acoustic waves in anisotropic materials. Ultrasonics 2000;38(1–8):232–6.
[45] Bucur V, Lanceleur P, Roge B. Acoustic properties of wood in tridimensional representation of slowness surfaces. Ultrasonics 2002; 40(1–8):537–41.
[46] Bucur V. Techniques for high resolution imaging of wood structure: a review. Meas Sci, Technol 2003;14(17):R91–R8.
[47] Lanceleur P, de Belleval JF, Mercier N. Synthetic tridimensional representation of slowness surfaces of anisotropic materials. Acta Acust united Ac 1998;84(11):1047–54.
[48] Maysenholder W. Sound transmission through periodically inhomogeneous anisotropic thin plates: generalizations of Cremer's thin plate theory. Acta Acust united Ac 1998;84(9):668–80.
[49] Carcione JM, Cavallini F, Helbig K. Anisotropic attenuation and material symmetry. Acta Acust united Ac 1998;84(3):495–502.
[50] Achenbach JD. Wave propagation in elastic solids. New York: North Holland; 1975.
[51] Dunn ML. Viscoelastic damping of particle and fiber reinforced composite materials. J Acoust Soc Am 1995;98(11):3360–74.
[52] Baudouin S, Hosten B. Immersion ultrasonic method to measure elastic constants and anisotropic attenuation in polymer-matrix and fiber-reinforced composite materials. Ultrasonics 1996;34:379–82.
[53] Vandenbossche B, Kriz RD, Oshima T. Stress-Wave displacement Polarizations and Attenuation in Unidirectional composites: theory and Experiment. Res Nondestr Eval 1996;8:101–23.
[54] Waters KR, Hughes MS, Mobley J, Brandenburger GH, Miller JG. On the applicability of Kramers-Krönig relations for ultrasonic attenuation obeying a frequency power law. J Acoust Soc Am 2000;108(2): 556–63.
[55] Moreno E, Acevedo P, Castillo M. Thickness measurement in composite materials using Lamb waves Viscoelastic effects. Ultrasonics 2000;37:595–9.
[56] Achenbach JD. Wave propagation in elastic solids. Amsterdam: North Holland, Elsevier Science Publishers; 1975.